Hydrogen deficiency in Ti-rich biotite from anatectic metapelites (El Joyazo, SE Spain): Crystal-chemical aspects and implications for high-temperature petrogenesis

BERNARDO CESARE,[1,*] GIUSEPPE CRUCIANI,[2] AND UMBERTO RUSSO[3]

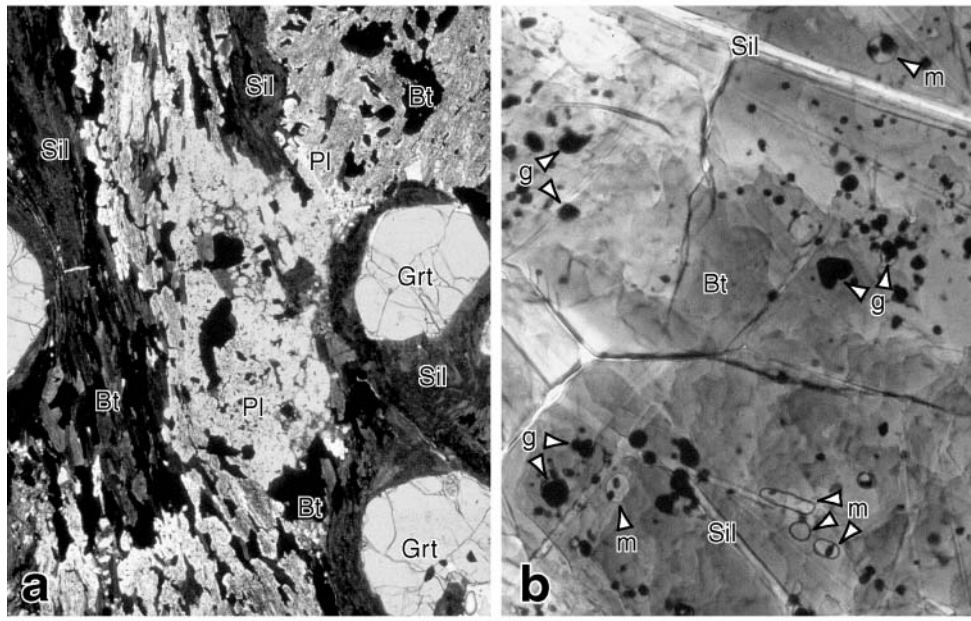

FIGURE 2. (**a**) Photomicrograph of a typical xenolith of El Joyazo, made of biotite (Bt), plagioclase (Pl) sillimanite (Sil) and garnet (Grt). (Plane-polarized light, width of view = 18 mm). (**b**) Photomicrograph of an inclusion-rich crystal of biotite. Inclusions consist primarily of rhyolitic glass (m), graphite (g), and sillimanite (s). (Plane-polarized light, width of view = 150 μm).

TABLE 2. H_2O concentrations (in wt%) recalculated from SIMS measurement of hydrogen

HO20		HO30		HO50	
Id	H_2O	Id	H_2O	Id	H_2O
HO20-3-1	2.61	HO30-2-1	2.54	HO50-4-1	2.24
HO20-3-2	2.59	HO30-2-2	2.70	HO50-4-2	2.42
HO20-3-3	2.53	HO30-2-3	2.61	HO50-4-3	2.36
HO20-3-4	2.31	HO30-2-4	2.55	HO50-4-4	2.51
HO20-3-5	2.61	HO30-2-5	2.41	HO50-4-5	2.66
HO20-3-6	2.53	HO30-2-6	2.45	HO50-4-6	2.65
HO20-3-7	2.42	HO30-2-7	2.60	HO50-4-7	2.59
HO20-3-8	2.68	HO30-3-1	2.51	HO50-4-8	2.50
HO20-3-9	2.54	HO30-3-2	2.34	HO50-3-1	2.69
HO20-3-1	2.56	HO30-3-3	2.49	HO50-3-2	2.80
HO20-3-2	2.70	HO30-3-4	2.47	HO50-3-3	3.31
HO20-3-3	2.75			HO50-3-4	3.34
HO20-3-4	2.86			HO50-3-5	3.22
HO20-3-5	2.48			HO50-3-6	3.19
HO20-3-6	2.28			HO50-3-7	3.07
HO20-3-10*	3.64			HO50-4-9	2.51
				HO50-4-10	2.53
				HO50-4-11	2.61
				HO50-4-12	2.41

Notes: Reported are all spot analyses from each sample.
* This value has not been considered for the calculation of average in Table 3 (see text for details).

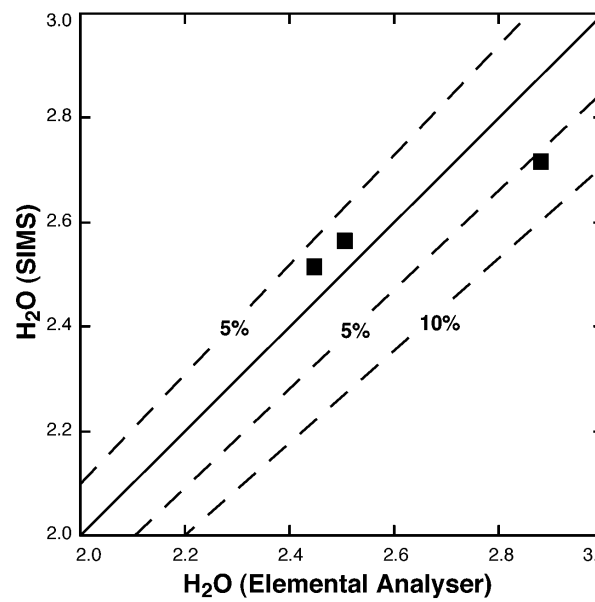

FIGURE 3. SIMS H_2O contents vs. C-H-N elemental analyzer data. Solid line defines 1/1 correlation. Dashed lines contour ±5% discrepancy.

TABLE 6. Mössbauer effecter parameters for samples HO30 and HO50 obtained by Lorentzian line profiles according to models b and c

		Fe^{2+}					Fe^{3+}				
	χ^2	δ (mm/s)	ΔE_Q (mm/s)	Γ (mm/s)	A (%)	A_-/A_+	δ (mm/s)	ΔE_Q (mm/s)	Γ (mm/s)	A (%)	A_-/A_+
HO30 b	1.580	1.123(3)	2.58(2)	0.26(2)	21(7)	0.97(4)	0.57(1)	0.62(3)	0.36(3)	10(2)	1*
		1.02(1)	2.28(2)	0.30(5)	36(9)	0.94(2)	0.41(1)	1.41(4)	0.30(5)	6(2)	1*
		1.081(4)	1.93(5)	0.40(3)	27(9)	1.00(2)					
HO30 c	3.819	1.118(3)	2.48(1)	0.31(1)	34(4)	0.98(9)	0.57(1)	0.63(2)	0.32(2)	9(1)	1*
		1.086(5)	2.12(2)	0.43(1)	53(5)	1.02(7)	0.44(2)	1.37(2)	0.24(3)	5(1)	1*
HO50 b	0.793	1.254(5)	2.57(2)	0.26(2)	28(8)	0.98(8)	0.55(2)	0.55(5)	0.27(5)	5(1)	1*
		1.108(4)	2.28(3)	0.30(6)	34(2)	0.97(7)	0.40(2)	1.34(6)	0.24(8)	4(1)	1*
		1.090(9)	1.92(5)	0.40(4)	29(8)	1.10(9)					
HO50 c	1.510	1.125(3)	2.49(1)	0.31(2)	41(5)	1.05(7)	0.56(1)	0.56(5)	0.22(5)	4(1)	1*
		1.107(6)	2.10(1)	0.44(2)	52(6)	0.97(6)	0.42(2)	1.31(5)	0.20(6)	3(1)	1*

* Value constrained during the fitting procedure.

TABLE 7. Mössbauer parameters for samples HO30 and HO50 obtained by quadrupole splitting distribution method according to models d and e

		Fe^{2+}													Fe^{3+}							
	χ^2	Γ (mm/s)	δ_0 (mm/s)	δ_1 (mm/s)	A_-/A_+	ΔE_Q (mm/s)	σ (%)	P	ΔE_Q (mm/s)	σ	P (%)	ΔE_Q (mm/s)	σ	P (%)	δ_0 (mm/s)	δ_1 (mm/s)	ΔE_Q (mm/s)	σ	P (%)	ΔE_Q (mm/s)	σ	P (%)
HO30 d	0.400	0.099	1.014	0.400	0.93	2.423	0.241	48	1.99	0.34	32				0.564	0*	0.602	0.31	9	0.814	0.099	1.014
															0.418	0*	1.36	0.42	10			
HO30 e	0.483	0.106	0.995	0.0483	0.95	2.543	0.16	24	2.245	0.13	28	1.94	0.28	32	0.566	0*	0.579	0.28	8	1.133	0.106	0.995
															0.390	0*	1.43	0.31	8			
HO50 d	0.649	0.109	1.019	0.0375	0.97	2.465	0.214	53	2.020	0.30	34				0.568	0*	0.644	0.30	9	1.508	0.59	4
HO50 e	0.590	0.115	1.019	0.0402	0.97	2.577	0.13	26	2.299	0.14	22	2.053	0.13	40	0.540	0*	0.530	0.17	5			
															0.413	0*	1.346					

* Value constrained during the fitting procedure.

TABLE 9. Crystal data, refinement details, and unit-cell parameter for the studied biotites

Samples	Dimensions (mm)	N_{obs}	R_{obs}	a (Å)	b (Å)	c (Å)	β (°)	V (Å^3)
HO20	0.07 × 0.05 × 0.02	503	5.2	5.336(1)	9.248(1)	10.179(1)	100.11(1)	494.5(1)
HO30	0.09 × 0.06 × 0.03	580	5.2	5.337(1)	9.248(1)	10.171(1)	100.09(1)	494.3(1)
HO50	0.12 × 0.10 × 0.03	645	3.7	5.345(1)	9.258(1)	10.198(1)	100.15(1)	496.7(1)

Note: $R_{obs} = \Sigma\ (|I F_o| - |F_c|I)/\Sigma\ F_o \times 100$ with $[F_o > 4\text{sig}(F_o)]$. Estimated standard deviations are parentheses.

TABLE 10. Final atomic fractional coordinates, and equivalent isotropic (Å^2) and anisotropic (Å) thermal displacement factors

Atom	*x/a*	*y/b*	*z/c*	U_{eq}	U_{11}	U_{22}	U_{33}	U_{23}	U_{13}	U_{12}
					HO20					
K	0.0	0.0	0.0	0.0315 (6)	0.0234 (10)	0.0313 (12)	0.0409 (12)	0.0	0.0087 (9)	0.0
T	0.5748 (2)	0.1668 (1)	0.2246 (1)	0.0118 (2)	0.0069 (4)	0.0123 (5)	0.0162 (4)	0.0001 (4)	0.0023 (3)	0.0002 (3)
M1	0.0	0.5	0.5	0.0117 (3)	0.0112 (6)	0.0082 (6)	0.0167 (6)	0.0	0.0053 (5)	0.0
M2	0.0	0.8365 (4)	0.5	0.0128 (2)	0.0081 (4)	0.0131 (5)	0.0171 (4)	0.0	0.0023 (3)	0.0
O1	0.8264 (5)	0.2299 (3)	0.1676 (3)	0.0234 (7)	0.0157 (12)	0.0287 (15)	0.0267 (13)	–0.0034 (12)	0.0059 (11)	–0.0090 (11)
O2	0.5146 (8)	0.0	0.1687 (4)	0.0242 (10)	0.0279 (20)	0.0139 (18)	0.0290 (20)	0.0	–0.0001 (17)	0.0
O3	0.6303 (5)	0.1685 (3)	0.3923 (3)	0.0184 (6)	0.0181 (13)	0.0203 (14)	0.0163 (11)	0.0014 (11)	0.0022 (10)	0.0002 (10)
O4	0.1343 (7)	0.0	0.3993 (4)	0.0179 (9)	0.0217 (18)	0.0181 (18)	0.0140 (16)	0.0	0.0034 (14)	0.0
H	0.178 (13)	0.0	0.314 (4)	0.0300						
					HO30					
K	0.0	0.0	0.0	0.0305 (5)	0.0254 (9)	0.0299 (10)	0.0376 (10)	0.0	0.0091 (8)	0.0
T	0.5745 (2)	0.1671 (1)	0.2242 (1)	0.0123 (2)	0.0095 (3)	0.0125 (4)	0.0150 (4)	0.0010 (4)	0.0028 (3)	–0.0006 (3)
M1	0.0	0.5	0.5	0.0123 (3)	0.0138 (5)	0.0082 (5)	0.0155 (5)	0.0	0.0040 (4)	0.0
M2	0.0	0.8368 (4)	0.5	0.0135 (2)	0.0097 (4)	0.0138 (4)	0.0170 (4)	0.0	0.0025 (3)	0.0
O1	0.8247 (5)	0.2298 (3)	0.1675 (2)	0.0231 (6)	0.0180 (11)	0.0281 (13)	0.0238 (11)	–0.0030 (11)	0.0050 (10)	–0.0080 (10)
O2	0.5152 (7)	0.0	0.1691 (4)	0.0244 (9)	0.0294 (19)	0.0171 (16)	0.0243 (17)	0.0	–0.0023 (15)	0.0
O3	0.6312 (5)	0.1678 (3)	0.3923 (2)	0.0179 (5)	0.0184 (10)	0.0188 (10)	0.0161 (10)	0.0016 (10)	0.0021 (8)	0.0005 (10)
O4	0.1334 (7)	0.0	0.3992 (3)	0.0202 (8)	0.0264 (17)	0.0196 (15)	0.0157 (15)	0.0	0.0070 (13)	0.0
H	0.123 (15)	0.0	0.307 (3)	0.0300						
					HO50					
K	0.0	0.0	0.0	0.0329 (6)	0.0314 (9)	0.0306 (10)	0.0368 (11)	0.0	0.0060 (7)	0.0
T	0.5748 (1)	0.1672 (1)	0.2251 (1)	0.0102 (2)	0.0104 (4)	0.0088 (4)	0.0114 (4)	0.0002 (3)	0.0018 (3)	–0.0004 (3)
M1	0.0	0.5	0.5	0.0097 (3)	0.0087 (5)	0.0065 (5)	0.0147 (6)	0.0	0.0039 (4)	0.0
M2	0.0	0.8370 (1)	0.5	0.0112 (3)	0.0073 (4)	0.0129 (4)	0.0134 (4)	0.0	0.0015 (3)	0.0
O1	0.8254 (4)	0.2304 (2)	0.1685 (2)	0.0208 (5)	0.0181 (10)	0.0255 (11)	0.0196 (10)	–0.0041 (9)	0.0053 (8)	–0.0068 (8)
O2	0.5174 (5)	0.0	0.1705 (2)	0.0202 (6)	0.0285 (15)	0.0127 (13)	0.0177 (14)	0.0	–0.0003 (12)	0.0
O3	0.6318 (4)	0.1693 (2)	0.3918 (2)	0.0162 (4)	0.0184 (10)	0.0180 (9)	0.0117 (9)	–0.0014 (7)	0.0015 (8)	–0.0003 (7)
O4	0.1304 (5)	0.0	0.3991 (3)	0.0192 (6)	0.0185 (14)	0.0243 (14)	0.0143 (14)	0.0	0.0017 (11)	0.0
H	0.117 (25)	0.0	0.303 (5)	0.0300						

Notes: The anisotropic displacement factor takes the form: $-2\pi^2[h^2a^{*2}U_{11} + k^2b^{*2}U_{22} + ... + 2hka^*b^*U_{12}]$. U_{eq} is defined as one third of the trace of the orthogonalized U_{ij} tensor. Estimated standard deviations in parentheses refer to the last digit.

TABLE 11. Selected bond distances (Å) for biotites of this study

Sample	HO20	HO30	HO50
	Tetrahedral layer		
T-O1	1.654(8)	1.650(4)	1.655(2)
T-O1'	1.659(8)	1.658(4)	1.656(2)
T-O2	1.656(4)	1.656(2)	1.655(1)
T-O3	1.680(5)	1.683(3)	1.674(2)
	1.663	1.662	1.660
	Octahedral layer		
M1-O4 (×2)	2.039(7)	2.044(4)	2.061(3)
M1-O3 (×4)	2.093(5)	2.090(3)	2.108(2)
	2.075	2.074	2.092
M2-O4 (×2)	2.027(5)	2.023(4)	2.019(2)
M2-O3 (×2)	2.082(5)	2.079(3)	2.081(2)
M2-O3' (×2)	2.090(5)	2.097(3)	2.097(2)
	2.066	2.066	2.065
	Interlayer		
K-O1 (×4)	2.973(8)	2.975(4)	2.990(2)
K-O1' (×4)	3.338(8)	3.334(4)	3.340(2)
K-O2 (×2)	2.972(11)	2.977(6)	2.996(3)
K-O2' (×2)	3.350(11)	3.348(6)	3.355(3)
<K-O_{inner}>	2.973	2.976	2.992
<K-O_{outer}>	3.342	3.339	3.345
	3.157	3.157	3.168

TABLE 12. Selected geometrical parameters calculated from structure analysis results

Sample	HO20	HO30	HO50
	Whole layer		
β_{ideal} (°)	100.06	100.07	100.06
Intralayer shift	–0.3349*a*	–0.3339*a*	–0.3362*a*
Δ_{TM} (Å)	0.559	0.557	0.542
	Tetrahedral sheet		
$Volume_T$ (Å^3)	2.358	2.354	2.347
BLD_T (%)	0.533	0.643	0.416
t_T (Å)	2.248	2.246	2.235
α (°)	8.06	7.94	7.72
Δ*z* (Å)	0.011	0.016	0.020
	Octahedral sheet		
$Volume_{M1}$ (Å^3)	11.666	11.659	11.948
BLD_{M1} (%)	1.161	0.991	1.002
ELD_{M1} (%)	5.600	5.603	5.707
$Volume_{M2}$ (Å^3)	11.535	11.537	11.539
BLD_{M2} (%)	1.280	1.390	1.510
ELD_{M2} (%)	5.429	5.445	5.196
$Shift_{M2}$ (Å)	0.029	0.032	0.034
O4-O4 (Å)	2.699	2.694	2.682
$t_{M(O3-O4)}$ (Å)	2.112	2.111	2.123
$t_{M(O3)}$ (Å)	2.159	2.157	2.172
$t_{M(O4)}$ (Å)	2.018	2.020	2.027
	Interlayer		
$Volume_{K\text{-}inner}$ (Å^3)	35.012	35.103	35.694
$\Delta_{K\text{-}O}$ (Å)	0.369	0.363	0.353
t_{int} (Å)	3.366	3.365	3.396
$t_{K\text{-}O4}$ (Å)	4.001	3.997	4.006

Notes: β_{ideal} = ideal monoclinic angle = $\cos^{-1}(-a/3c)$; intralayer shift = $c\cos\beta/a$; Δ_{TM} = dimensional misfit = $2\sqrt{3}$<O-O>$_{basal}$–$3\sqrt{2}$ (<M1-O> + 2<M2-O>)/3; α = tetrahedral in-001-plane rotation angle = | 120° – <O_b-O_b-O_b> |/2 where <O_b-O_b-O_b> is the mean angle between basal edges of neighboring tetrahedra in the ring; Δ*z* = basal corrugation = ($z_{O2} - z_{O1}$)*c*sinb; BLD = bond length distortion = 100/n * Σ_i |(M-O)$_i$-<M-O>|/<M-O>; ELD = edge length distortion = 100/n * Σ_i |(O-O)$_i$ – <O-O>|/<O-O>; $Shift_{M2}$ = off-center shift of the M2 cation defined as the distance between the refined position of cation and the geometrical center of M2 (coordinates: *x*/*a* = 0.0, *y*/*b* = 0.8333, *z*/*c*=0.5); $\Delta_{K\text{-}O}$ = (<K-O_{inner}> – <K-O_{outer}>); t_T = tetrahedral sheet thickness calculated from the *z* coordinates of basal and apical O atoms; $t_{M(O3\text{-}O4)}$, $t_{M(O3)}$, $t_{M(O4)}$ = octahedral sheet thickness calculated from the *z* coordinates, respectively, of all oxygens bonded to octahedral cations (O3 and O4), of only the tetrahedral apical oxygens (O3), and of only oxygens bonded to hydrogens (O4); t_{int} = interlayer sheet thickness from the *z* coordinates of basal O atoms; $t_{K\text{-}O4}$ = projection of K-O4 distance along c*.

TABLE 13. Octahedral cation distribution from least-square minimization

Octahedral sites	
Sample:	Octahedral cation distribution
HO20	M1:($Mg_{0.272}Fe^{2+}_{0.477}Fe^{3+}_{0.215}Mn_{0.003}\square_{0.034}$)
	M2:($Mg_{0.235}Fe^{2+}_{0.424}Al_{0.208}Ti_{0.132}Cr_{0.001}$)
HO30	M1:($Mg_{0.239}Fe^{2+}_{0.456}Fe^{3+}_{0.247}Mn_{0.004}\square_{0.054}$)
	M2:($Mg_{0.245}Fe^{2+}_{0.420}Al_{0.197}Ti_{0.136}Cr_{0.002}$)
HO50	M1:($Mg_{0.329}Fe^{2+}_{0.551}Fe^{3+}_{0.107}Mn_{0.003}\square_{0.017}$)
	M2:($Mg_{0.205}Fe^{2+}_{0.413}Fe^{3+}_{0.023}Al_{0.213}Ti_{0.143}Cr_{0.002}$)

Sample:	HO20	HO30	HO50
	M1 octahedron		
M1 $e^-_{X\text{-}ref}$	19.69	19.84	20.23
M1 e^-_{calc}	21.32	21.25	21.14
<M1-O>$_{X\text{-}ref}$ (Å)	2.075	2.074	2.092
<M1-O>$_{calc}$ (Å)	2.086	2.085	2.090
	M2 octahedron		
M2 $e^-_{X\text{-}ref}$	19.71	19.70	19.39
M2 e^-_{calc}	19.48	19.45	19.77
<M2-O>$_{X\text{-}ref}$ (Å)	2.066	2.066	2.065
<M2-O>$_{calc}$ (Å)	2.061	2.062	2.060
$\Sigma e^-_{(M1 + 2M2)\ X\text{-}ref}$	59.11	59.24	59.02
$\Sigma e^-_{(M1 + 2M2)\ EPMA}$	60.28	60.15	60.69
	Interlayer site		
K $e^-_{X\text{-}ref}$	17.01	17.37	16.90
K e^-_{EPMA}	16.34	16.44	17.05
	Tetrahedral site		
<T-O>$_{X\text{-}ref}$ (Å)	1.663	1.663	1.660
<T-O>$_{EPMA}$ (Å)	1.661	1.661	1.661

Notes: Observed and calculated octahedral and tetrahedral mean distances. Observed and calculated mean atomic numbers of octahedral and interlayer sites. e^- = mean atomic number. Octahedral cation distribution was calculated by the minimization procedure. Subscripts "X-ref", "EPMA", and "calc" refer to values as obtained from structure refinement, chemical analysis and minimization procedure, respectively. Ideal values for $^{[VI]}$M-O average bond distances (where $^{[VI]}$M = Mg, Fe^{2+}, Fe^{3+}, Al, Mn, Cr, Ti, □). <Si-O>$_{ideal}$ = 1.618 Å and <$^{[IV]}$Al-O>$_{ideal}$=1.748 Å.

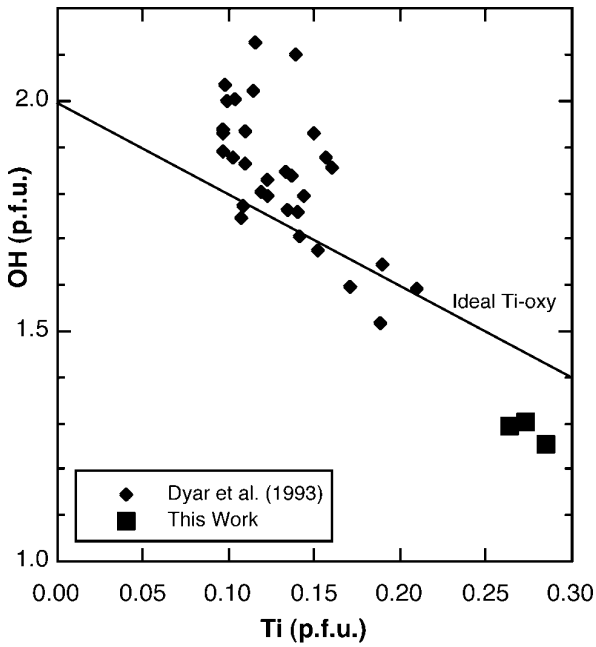

FIGURE 7. OH vs. Ti diagram. Symbols as in Figure 6. Solid line = model $Ti(OH)_{-2}$ exchange as in the Ti-oxy substitution.

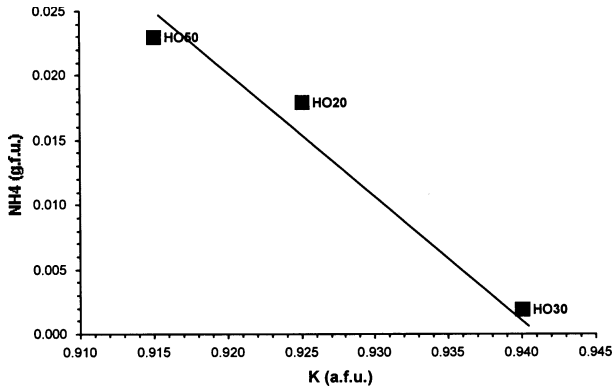

FIGURE 9. NH_4 vs. K diagram for the studied biotites. Alignment of data parallel to the 1:1 line supports the occurrence of the $(NH_4)(K,Na)_{-1}$ exchange.

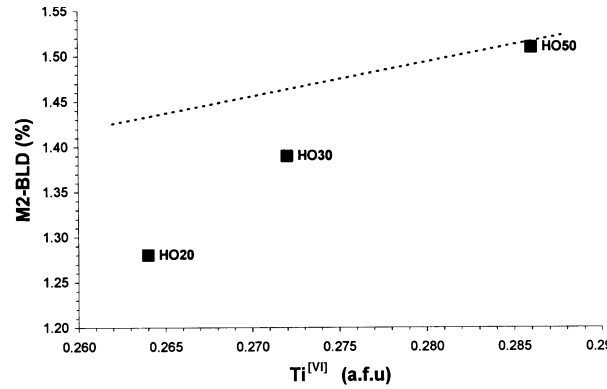

FIGURE 12. Plot of the bond-length distortion parameter (BLD) of the M2 octahedral site vs. ^{VI}Ti content. The dotted line represents the equation $(BLD_{M2}) = 0.43(8) + {}^{[VI]}Ti \times 3.8(3)$ ($N_{obs} = 24$, $R^2 = 0.78$) obtained by regression on data from Cruciani and Zanazzi (1994).